

The structural diversity of Te–I interactions within tetraorganoditelluroxane diiodides and related compounds

Jens Beckmann*, Jens Bolsinger, Johann Spandl

Institut für Chemie und Biochemie, Freie Universität Berlin, Fabeckstraße 34–36, 14195 Berlin, Germany

Received 22 October 2007; received in revised form 3 December 2007; accepted 6 December 2007

Available online 15 December 2007

Abstract

Two tetraorganoditelluroxane diiodides ($(R_2Te)_2OI_2$ (**3**, $R = p\text{-MeOC}_6\text{H}_4$; **5**, $R = \text{Me}$) were prepared by the reaction of ($p\text{-MeOC}_6\text{H}_4$)₂TeI₂ (**1**) and ($p\text{-MeOC}_6\text{H}_4$)₂TeO (**2**) and the base hydrolysis of Me₂TeI₂ (**4**), respectively. The base hydrolysis of C₄H₈TeI₂ (**8**) afforded the tritelluroxane diiodide (C₄H₈Te)₃O₂I₂ (**9**). The reaction of Me₂TeI₂ (**4**) and Me₂Te(OH)₂ (**6**) in a ratio of 1:3 produced the coordination polymer of the composition 2 (Me₂Te)₂O(I)OH · H₂O (**7**). An attempt at preparing an adduct of **3** with iodine failed but provided co-crystals of ($p\text{-MeOC}_6\text{H}_4$)₂TeI₂ · ½I₂ (**1a**). The supramolecular structures of **1a**, **3**, **5**, **7** and **9** are dominated by structurally directing secondary Te···I interactions.

© 2007 Elsevier B.V. All rights reserved.

Keywords: Tellurium; Secondary bonding; Supramolecular structure

1. Introduction

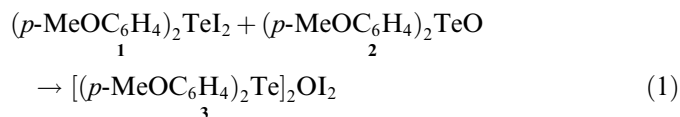
The coordination chemistry of organotellurium compounds has attracted considerable attention in recent years due to a fascinating wealth of molecular and supramolecular structures [1]. The diversity encountered within these structures can be attributed to the fact that tellurium can adopt different equally stable valence states and coordination modes, which are often closely associated with hypervalent and/or secondary bonding. Interactions between tellurium and iodine are of particular interest as the electronegativity and size difference of these elements are only marginal. The organotellurenyl group has even substantial pseudohalide character and is interchangeable with iodine in many structures (e.g. I₂ vs. RTeI, RTeI · I₂; ICl vs. RTeCl; I₃[−] vs. RTeI₂[−], (RTe)₃[−]) [2]. Organotellurium(IV) iodides were extensively investigated by variation of the number and size of the organic substituents and the supra-

molecular motifs observed were rationalized by the concepts of crystal engineering [3].

In preceding work we were interested in the structure [4] and reactivity of telluroxanes [5]. In this context we have now structurally investigated two tetraorganoditelluroxane diiodides and three related compounds showing a number of structurally directing secondary Te···I interactions.

2. Discussion

The redistribution reaction of equimolar amounts of ($p\text{-MeOC}_6\text{H}_4$)₂TeI₂ (**1**) and ($p\text{-MeOC}_6\text{H}_4$)₂TeO (**2**) produced the tetraorganoditelluroxane diiodide [($p\text{-MeOC}_6\text{H}_4$)₂Te]₂OI₂ (**3**) in almost quantitative yield as orange crystalline solid



The molecular structure of [($p\text{-MeOC}_6\text{H}_4$)₂Te]₂OI₂ (**3**) is shown in Fig. 1. Selected bond parameters and crystal and refinement data are collected in the caption of Fig. 1

* Corresponding author.

E-mail address: beckmann@chemie.fu-berlin.de (J. Beckmann).

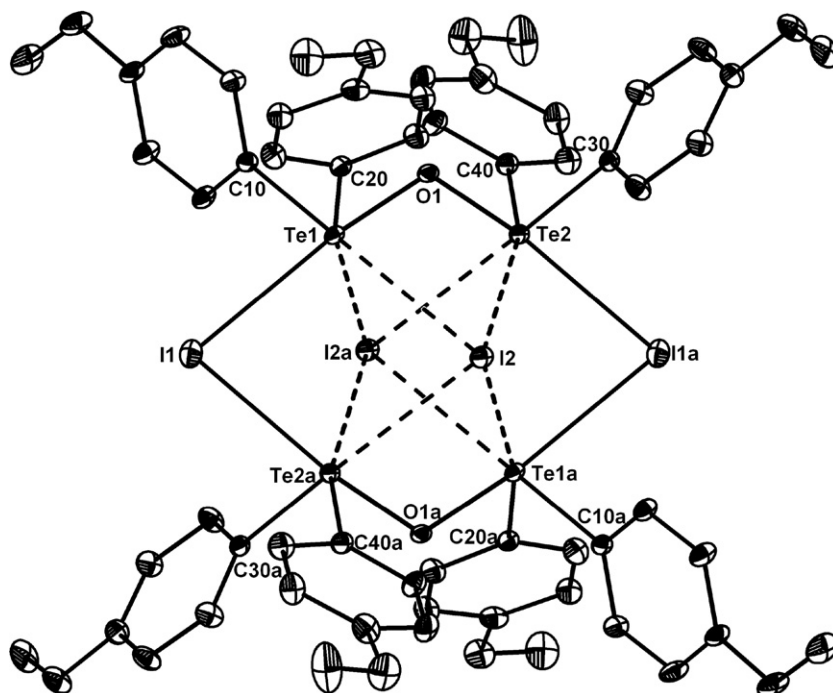


Fig. 1. Molecular structure and supramolecular association of $[(p\text{-MeOC}_6\text{H}_4)_2\text{Te}]_2\text{OI}_2$ (**3**) showing 30% probability ellipsoids and the crystallographic numbering scheme. The CHCl_3 molecules have been omitted for clarity. Symmetry code used to generate equivalent atoms: $a = 1 - x, 1 - y, 1 - z$. Selected bond parameters [$\text{\AA}, ^\circ$]: Te1–C10 2.107(7), Te1–C20 2.102(7), Te1–I1 3.294(2), Te1 \cdots I2 3.499(2), Te1 \cdots I2a 3.696(1), Te1–O1 1.989(6), Te2–C30 2.116(8), Te2–C40 2.119(8), Te2–I1a 3.262(2), Te2 \cdots I2 3.740(2), Te2 \cdots I2a 3.513(2), Te2–O1 1.982(6); O1–Te1–I1 174.2(2), O1–Te2–I1a 173.4(2), Te1–O1–Te2 118.8(2).

and Table 1, respectively. The structure of **3** can be described as two centrosymmetric $\text{R}_2\text{TeOTeR}_2$ units that are linked by four iodine atoms. Taking into account the stereochemically active lone pair, the spatial arrangement around the Te atoms is trigonal bipyramidal with a C_2IO donor set and the expected ligand occupancies. The average axial Te–I bond lengths of 3.278(2) \AA are considerably longer than those of $(p\text{-MeOC}_6\text{H}_4)_2\text{TeI}_2$ (**1**) being 2.9234(8) \AA [6]. In turn, the Te–O bond lengths of 1.986(6) \AA are somewhat shorter than the Te–O ‘single bonds’ of the polymeric parent $[(p\text{-MeOC}_6\text{H}_4)_2\text{TeO}]_n$ (**2**) being 2.063(2) \AA [4]. Thus, unlike the two starting materials **1** and **2**, the axial coordination of **3** is somewhat asymmetric. A similar observation was made for related trigonal bipyramidal triorganostannate anions having two unequal axial ligands [7]. In addition to the two axial I atoms (I1, I1a), there are two I atoms (I2, I2a) associated with the Te atoms *via* longer secondary interactions of average 3.612(2) \AA . In this way, the overall crystal structure of **3** closely resembles that of the tetraorganoditelluroxane ditriflate $[(p\text{-MeOC}_6\text{H}_4)_2\text{Te}]_2\text{O}(\text{O}_3\text{SCF}_3)_2$ [8]. The Te–O–Te angle of **3** being 118.8(2) $^\circ$ compares well with the corresponding angle in $[(p\text{-MeOC}_6\text{H}_4)_2\text{Te}]_2\text{O}(\text{O}_3\text{SCF}_3)_2$ (120.2(3) $^\circ$) and related tetraorganoditelluroxanes [8]. The primary coordination sphere of **3** is also reminiscent of the molecular structure of hexaphenyldistiboxane diiodide $(\text{Ph}_3\text{Sb})_2\text{OI}_2$ [9]. In solution **3** was characterized by ^1H and ^{13}C NMR spectroscopy (Section 3), however, all attempts at obtaining a ^{125}Te NMR signal failed. A similar

observation was made previously for $[(p\text{-MeOC}_6\text{H}_4)_2\text{TeO}]_n$ (**2**) [4].

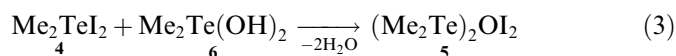
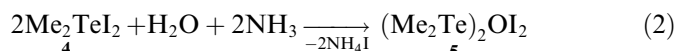
The hexaphenyldistiboxane diiodide $(\text{Ph}_3\text{Sb})_2\text{OI}_2$ is known to form an adduct with molecular iodine in the solid state, namely $(\text{Ph}_3\text{Sb})_2\text{OI}_2 \cdot \frac{1}{4}\text{I}_2$ [10]. When we attempted the preparation of a similar complex of $[(p\text{-MeOC}_6\text{H}_4)_2\text{Te}]_2\text{OI}_2$ (**3**) and iodine, we surprisingly obtained co-crystals of $(p\text{-MeOC}_6\text{H}_4)_2\text{TeI}_2 \cdot \frac{1}{2}\text{I}_2$ (**1a**) in about 30% yield as black crystals. The same material was obtained nearly quantitatively when stoichiometric amounts of **1** and iodine were co-crystallized. To the best of our knowledge, there are only three adducts of dialkyltellurium diiodides with iodine, namely $\text{Me}_2\text{TeI}_2 \cdot \text{I}_2$ [11], $\text{C}_5\text{H}_{10}\text{TeI}_2 \cdot \text{I}_2$, $\text{C}_4\text{H}_8\text{TeI}_2 \cdot \frac{1}{2}\text{I}_2$ [12]. The crystal structure of $(p\text{-MeOC}_6\text{H}_4)_2\text{TeI}_2 \cdot \frac{1}{2}\text{I}_2$ (**1a**) is shown in Fig. 2. Selected bond parameters and crystal and refinement data are collected in the caption of Fig. 2 and Table 1, respectively. The crystal structure of **1a** consists of a centrosymmetric tetramer made of $(p\text{-MeOC}_6\text{H}_4)_2\text{TeI}_2$ molecules, which are associated *via* secondary $\text{Te}\cdots\text{I}$ interactions. The bond parameters and the supramolecular arrangement of the tetramer are virtually identical with those of the two known polymorphs of $(p\text{-MeOC}_6\text{H}_4)_2\text{TeI}_2$ (**1**) [6]. The iodine molecule of **1a** links adjacent tetramers in the crystal lattice *via* $\text{I}\cdots\text{I}$ contacts of average 3.360(1) \AA . The primary I–I bond lengths of 2.743(1) \AA is similar to those of other iodine adducts, such as $\text{Me}_2\text{TeI}_2 \cdot \text{I}_2$ (2.756(2) \AA) [11], $\text{C}_5\text{H}_{10}\text{TeI}_2 \cdot \text{I}_2$ (2.744(1) \AA), $\text{C}_4\text{H}_8\text{TeI}_2 \cdot \frac{1}{2}\text{I}_2$ (2.759(1) \AA) [12] and $(\text{Ph}_3\text{Sb})_2\text{OI}_2 \cdot \frac{1}{4}\text{I}_2$ (2.732(3) \AA) [10]. The motif

Table 1
Crystallographic data and refinement details for **3**, **1a**, **5**, **7** and **9**

	3	1a	5	7	9
Formula	C ₂₈ H ₂₈ I ₂ O ₅ Te ₂ · CHCl ₃	C ₂₈ H ₂₈ I ₄ O ₄ Te ₂ · I ₂	C ₄ H ₁₂ I ₂ O ₂ Te ₂	C ₈ H ₂₂ I ₂ O ₄ Te ₄ · H ₂ O	C ₁₂ H ₂₄ I ₂ O ₂ Te ₃
Formula weight	1072.87	1445.10	585.14	965.48	836.91
Crystal system	Triclinic	Triclinic	Orthorhombic	Orthorhombic	Orthorhombic
Crystal size (mm ³)	0.36 × 0.20 × 0.05	0.73 × 0.12 × 0.05	0.33 × 0.26 × 0.17	0.20 × 0.18 × 0.05	0.68 × 0.25 × 0.15
Temperature (K)	173	173	173	173	150
Space group	<i>P</i> $\bar{1}$	<i>P</i> $\bar{1}$	<i>Pbca</i>	<i>Pbca</i>	<i>P</i> 2 ₁ 2 ₁
<i>a</i> (Å)	10.828(5)	11.158(5)	16.041(4)	12.269(2)	9.712(4)
<i>b</i> (Å)	12.311(6)	13.552(5)	15.587(4)	14.131(3)	10.483(4)
<i>c</i> (Å)	14.229(7)	14.284(5)	21.001(5)	26.350(5)	20.230(8)
α (°)	70.935(10)	63.933(5)	90	90	90
β (°)	89.197(12)	85.830(5)	90	90	90
γ (°)	74.478(9)	77.065(5)	90	90	90
<i>V</i> (Å ³)	1721.7(14)	1890.2(13)	5251(2)	4568.3(14)	2059.8(14)
<i>Z</i>	2	2	16	8	4
<i>D</i> _c (g cm ⁻³)	2.069	2.539	2.961	2.805	2.699
<i>F</i> (000)	1008	1300	4064	3408	1496
μ (Mo K α , mm ⁻¹)	3.755	6.472	9.101	7.770	7.216
Index ranges	-11 ≤ <i>k</i> ≤ 15, -17 ≤ <i>l</i> ≤ 17, -18 ≤ <i>h</i> ≤ 20	-15 ≤ <i>k</i> ≤ 15, -19 ≤ <i>l</i> ≤ 16, -20 ≤ <i>h</i> ≤ 19	-22 ≤ <i>k</i> ≤ 21, -18 ≤ <i>l</i> ≤ 22, -29 ≤ <i>h</i> ≤ 29	-17 ≤ <i>k</i> ≤ 14, -20 ≤ <i>l</i> ≤ 20, -37 ≤ <i>h</i> ≤ 26	-11 ≤ <i>k</i> ≤ 9, -12 ≤ <i>l</i> ≤ 9, -24 ≤ <i>h</i> ≤ 23
Measured data	19 680	23 293	61 885	53 877	6628
2 θ Range (°)	1.82–30.64	1.86–27.54	1.94–30.55	2.27–30.55	2.80–25.00
Completeness to θ_{\max} (%)	95.1	96.5	99.3	99.2	99.4
Unique data	10 129	11 192	7992	6944	3563
(<i>I</i> ≥ 2 θ (<i>I</i>))	7193	8239	6684	5860	3344
Number of refined parameters	370	361	163	176	172
Goodness-of-fit (<i>R</i> ²)	1.068	1.031	1.093	1.028	1.016
<i>R</i> , observed data; all data	0.0599; 0.0959	0.0327; 0.0556	0.0231; 0.0331	0.0276; 0.0369	0.0657; 0.0686
<i>R</i> _w , observed data; all data	0.1541; 0.1791	0.0692; 0.0781	0.0508; 0.0560	0.0666; 0.0722	0.1743; 0.1767
Largest diffraction peak/hole (e Å ⁻³)	4.166/–2.354	1.382/–1.396	1.205/–1.577	2.351/–1.359	2.844/–2.390

I1···I5–I6···I3 is also strongly reminiscent of ‘classical’ tetraiodide (2⁻) moieties found in numerous crystal structures. The Raman spectrum of solid (*p*-MeOC₆H₄)₂TeI₂ · ½I₂ (**1a**) reveals a band at $\tilde{\nu} = 176$ cm⁻¹ for the I–I stretching vibration, that compares well with that of (Ph₃Sb)₂OI₂ · ¼I₂ (174 cm⁻¹) [10]. In molecular iodine the same vibration was observed in the solid state at $\tilde{\nu} = 184$ cm⁻¹ and in the gas phase at $\tilde{\nu} = 213$ cm⁻¹ [13].

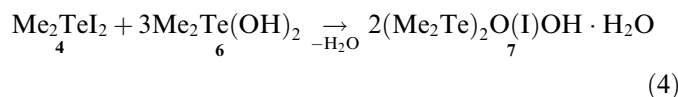
In pioneering work, Vernon prepared an analogue of **3**, namely the tetraorganoditelluroxane (Me₂Te)₂OI₂ (**5**), by the partial hydrolysis of Me₂TeI₂ (**4**) in aqueous ammonia (Eq. (2)), or alternatively, by the redistribution reaction of Me₂TeI₂ (**4**) and Me₂Te(OH)₂ (**6**), which proceeds with condensation of the hydroxyl groups (Eq. (3)) [14]. Since compound **5** was not completely characterized at the time, we repeated its synthesis and now report on full structural details



The crystal and molecular structure of (Me₂Te)₂OI₂ (**5**) is shown in Fig. 3. Selected bond parameters and crystal and refinement data are collected in the caption of Fig. 3 and Table 1, respectively. The structure contains two crys-

tallographically independent molecules of **5**, which are associated *via* intermolecular secondary Te···I interactions giving rise to the formation of a coordination polymer. The spatial arrangement around the four independent Te atoms resembles the distorted trigonal bipyramid observed for **3**. The mean Te–I bond lengths 3.167(6) Å is significantly longer than those of Me₂TeI₂ (2.925(3) Å) [15]. The secondary Te···I contacts of average 3.740(3) Å connecting adjacent molecules are somewhat longer than those of **3**.

According to Vernon the redistribution reaction of Me₂TeI₂ (**4**) and Me₂Te(OH)₂ (**6**) in a ratio of 1:2 produced a different product, namely the hexaorganotritelluroxane (Me₂Te)₃O₂I₂ (**5a**) [14]. When we attempted to reproduce the preparation of **5a**, we obtained a crystalline product of the composition 2 (Me₂Te)₂O(I)OH·H₂O (**7**) in good yield, which has a melting point similar to **5a**. However, formally compound **7** is the product of a redistribution reaction between Me₂TeI₂ (**4**) and Me₂Te(OH)₂ (**6**) in a ratio of 1:3



The crystal structure of **7** and a perspective view along the crystallographic *b*-axis are shown in Figs. 4 and 5. Selected bond parameters and crystal and refinement data are collected in the caption of Fig. 4 and Table 1, respectively.

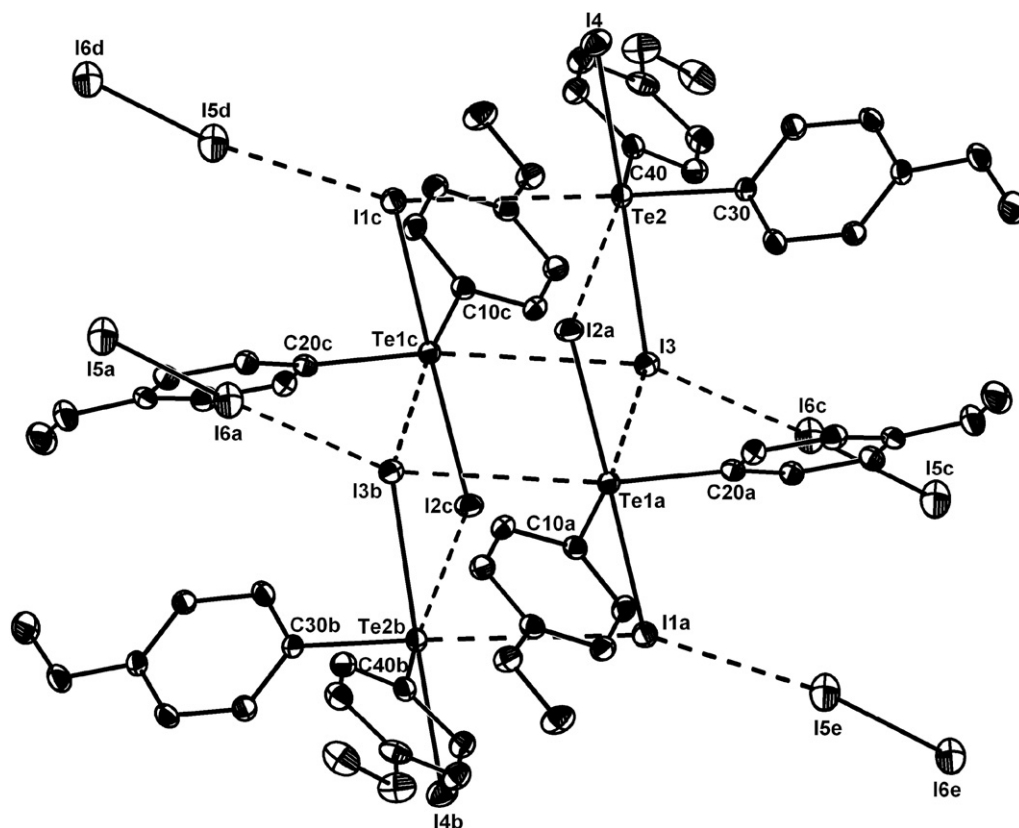


Fig. 2. Molecular structure and supramolecular association of $(p\text{-MeOC}_6\text{H}_4)_2\text{TeI}_2 \cdot \frac{1}{2}\text{I}_2$ (**1a**) showing 30% probability ellipsoids and the crystallographic numbering scheme. Symmetry codes used to generate equivalent atoms: $a = 1 - x, 1 - y, 1 - z, b = -x, 1 - y, 1 - z, c = -1 + x, y, z, d = -1 + x, y, 1 + z, e = 1 - x, 1 - y, -z$. Selected bond parameters [$\text{\AA}, \text{\circ}$]: Te1a–C10a 2.135(4), Te1a–C20a 2.134(4), Te1a–I1a 2.9818(8), Te1a–I2a 2.8964(7), Te1a \cdots I3 3.678(1), Te1a \cdots I3b 3.739(1), Te2–C30 2.115(4), Te2–C40 2.119(4), Te2–I3 3.0398(8), Te2–I4 2.8334(8), Te2 \cdots I1c 3.832(1), Te2 \cdots I2a 3.949(1), I1c \cdots I5a 3.492(1), I3 \cdots I6c 3.360(1), I5a–I6a 2.743(1); I1–Te1–I2 174.74(1), I3–Te2–I4 176.56(1).

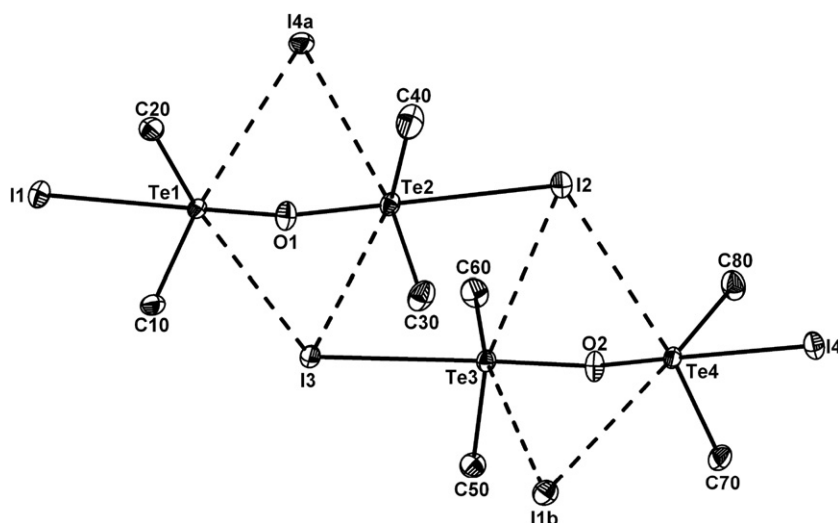


Fig. 3. Molecular structure and supramolecular association of $(\text{Me}_2\text{Te})_2\text{OI}_2$ (**5**) showing 30% probability ellipsoids and the crystallographic numbering scheme. Symmetry code used to generate equivalent atoms: $a = x, 0.5 - y, -0.5 + z, b = 0.5 - x, 1 - y, -0.5 + z$. Selected bond parameters [$\text{\AA}, \text{\circ}$]: Te1–C10 2.121(4), Te1–C20 2.107(4), Te1–I1 3.1854(7), Te1 \cdots I3 3.7083(7), Te1 \cdots I4a 3.6268(8), Te1–O1 1.976(3), Te2–C30 2.115(4), Te2–C40 2.108(5), Te2–I2 3.1692(6), Te2 \cdots I3 3.758(1), Te2 \cdots I4a 3.6066(8), Te2–O1 1.983(3), Te3–C50 2.105(4), Te3–C60 2.110(4), Te3–I3 3.1517(6), Te3 \cdots I2 3.7808(9), Te3 \cdots I1b 3.7756(8), Te3–O2 1.979(3), Te4–C70 2.115(4), Te4–C80 2.115(4), Te4–I4 3.1618(6), Te4 \cdots I1b 3.7503(9), Te4 \cdots I2 3.7503(9), Te4–O2 1.969(3), O1–Te1–I2 170.96(8); O1–Te2–I2 174.47(8), O2–Te3–I3 172.67(8), O2–Te4–I4 171.92(8), Te1–O1–Te2 123.5(1), Te3–O2–Te4 123.8(1).

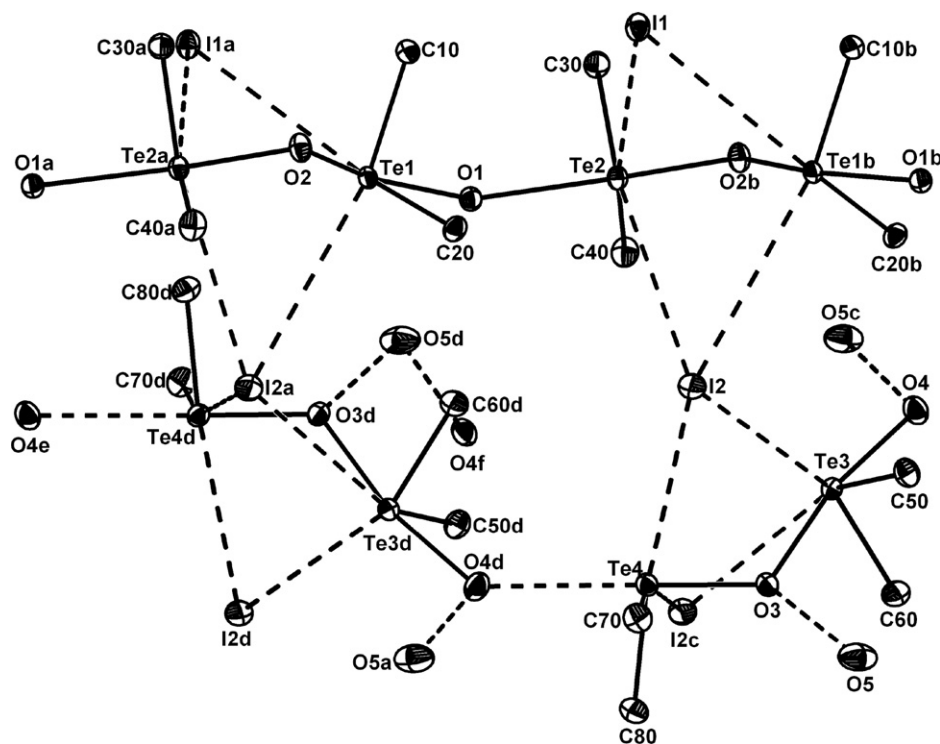


Fig. 4. Molecular structure and supramolecular association of **2** ($\text{Me}_2\text{Te})_2\text{O}(\text{I})\text{OH} \cdot \text{H}_2\text{O} (**7**) showing 30% probability ellipsoids and the crystallographic numbering scheme. Symmetry codes used to generate equivalent atoms: $a = 0.5 - x, 0.5 + y, z$, $b = 0.5 - x - 0.5 + y, z$, $c = 0.5 + x, y, 0.5 - z$, $d = 1 - x, 0.5 + y, 0.5 - z$, $e = x, 1 + y, z$, $f = 1.5 - x, 0.5 + y, z$. Selected bond parameters [\AA , $^\circ$]: Te1–O1 2.179(3), Te1–O2 2.039(3), Te1···I1a 3.802(1), Te1···I2a 3.916(1), Te1–C10 2.105(4), Te1–C20 2.104(4), Te2–O1 2.373(3), Te2–O2b 1.965(3), Te2···I1 3.667(1), Te2···I2 3.808(1), Te2–C30 2.112(4), Te2–C40 2.108(5), Te3–O3 2.195(3), Te3–O4 2.063(3), Te3···I2 4.099(1), Te3···I2c 4.193(1), Te3–C50 2.102(5), Te3–C60 2.097(5), Te4–O3 1.913(3), Te4···O4d 2.715(3), Te4···I2 3.702(1), Te4···I2c 4.147(1), Te4–C70 2.109(5), Te4–C80 2.111(5), O3···O5 2.785(6), O4···O5c 2.792(6); O1–Te1–O2 163.0(1), O1–Te1–C10 84.9(2), O2–Te1–C20 81.8(1), O2–Te1–C10 87.0(2), O2–Te1–C20 84.8(2), C10–Te1–C20 100.2(2), O1, Te2–O2b 172.0(1), O1–Te2–C40 84.2(2), O1–Te2–C30 85.4(1), O2b–Te2–C30 89.6(2), O2b–Te2–C40 90.1(2), C30–Te2–C40 94.3(2), O3–Te3–O4 167.6(1), O3–Te3–C50 84.6(2), O3–Te3–C60 82.4(2), O4–Te3–C50 86.6(2), O4–Te3–C60 90.0(2), C50–Te3–C60 96.5(2), O3–Te4–O4d 177.7(1), O3–Te4–C70 95.25(17), O3–Te4–C80 95.23(16), O4d–Te4–C70 82.5(2), O4d–Te4–C80 84.9(1), C70–Te4–C80 91.9(2), Te1–O1–Te2 131.1(1), Te1–O2–Te2a 120.8(2), Te3–O3–Te4 118.7(1), Te3–O4d–Te3d 130.3(1).$

The structure is complex and essentially contains two 1D polymers with a Te–O backbone. The first polymer string (Te1, O1, and Te2) can be regarded as $(\text{Me}_2\text{TeO})_n$ polymer, similar as the polymeric structure of $[(p\text{-MeOC}_6\text{H}_4)_2\text{TeO}]_n$ (**2**) [4]. The average Te–O bond length and the Te–O–Te angle are 2.139(3) \AA and $126.0(2)^\circ$ and compare well with the related values of **2** being 2.063(2) \AA and $126.0(1)^\circ$ [4]. Notably, the structures of $\text{Me}_2\text{Te}(\text{OH})_2$ (**6**) and potential condensation products, such as $(\text{Me}_2\text{TeO})_n$ (**6a**) are still unknown. The second polymer string (Te3, O3, Te4, and O4) comprises $\text{R}_2\text{Te}(\text{OH})\text{TeR}_2(\text{OH})$ units that are associated by short secondary Te···O(H) interactions of 2.373(3) \AA . The short Te–O(H) bonds within the $\text{R}_2\text{Te}(\text{OH})\text{TeR}_2(\text{OH})$ units are with average 2.058(3) \AA comparable with other ‘Te–O’ single bonds [4,5]. The two crystallographically independent iodide ions are surprisingly not involved in primary bonding to the Te atoms. However, they appear to play an integral role for the supramolecular association as they form secondary bonds to all Te atoms. The supramolecular arrangement of **7** is shown in Fig. 4. The lengths of secondary Te···I bonds vary between 3.667(1) and 4.193(1) \AA . The latter value is slightly larger than the sum of van-der Waals radii (4.04 \AA), however, the directionality

of the bonds suggests this to be an attractive interaction. The structural directing effect of the iodide ions is reminiscent of the recently reported dodecanuclear isopropyltellurium(IV)oxo cluster $[\text{Li}(\text{THF})_4][\{(i\text{-PrTe})_{12}\text{O}_{16}\text{Br}_4\{\text{Li}(\text{THF})\text{Br}\}_4\}\text{Br}] \cdot 2 \text{ THF}$, in which 8 Te atoms are situated around a structurally directing bromide ion [16]. The water molecule (O5) of **7** acts twice as acceptor for hydrogen bonds with the hydroxyl groups (O3, O4). The mean O···O distance of 2.788(6) is indicative for medium strength hydrogen bonding [17]. The IR spectrum of **7** confirms the presence of different hydroxy groups being involved in hydrogen bonding by showing three OH stretching vibrations at $\tilde{\nu} = 3433, 3302, 3221 \text{ cm}^{-1}$. Once isolated from aqueous solution, the solubility of **5** and **7** in water is very poor. The ^1H NMR spectra (D_2O) of **5** and **7** exhibit a signal resonance at δ 2.62 and 2.50 with tellurium satellites ($^2J(^1\text{H}\text{--}^{125}\text{Te}) = 26$ and 25 Hz). The simplicity of the ^1H NMR spectra suggests that the Te atoms are equal in solution, presumably due to electrolytic dissociation of **5** and **7**. In organic solvents **5** and **7** are virtually insoluble. It should be noted that an alternative (formal) description of **2** ($\text{Me}_2\text{Te})_2\text{O}(\text{I})\text{OH} \cdot \text{H}_2\text{O} (**7**) may be $\text{Me}_2\text{TeO} \cdot [\text{Me}_2(\text{I})\text{TeOTe}(\text{OH})] \cdot [\text{H}_3\text{O}]^+$, however, the$

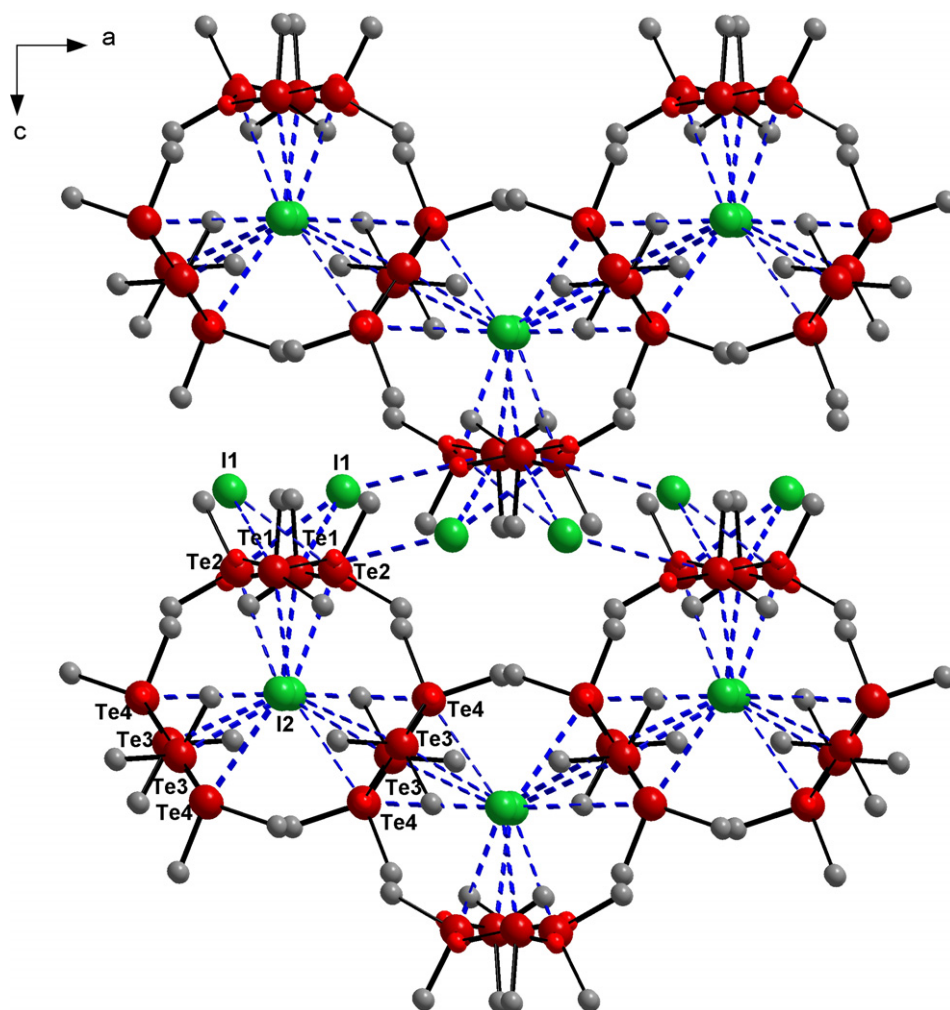
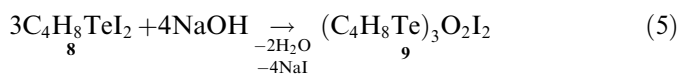


Fig. 5. Perspective view along the crystallographic *b*-axis of 2 (Me₂Te)₂O(I)OH · H₂O (**7**) showing the association of the 2D-polymer strings by secondary Te···I interactions (blue broken bonds).

aqueous solution of **7** reacts basic, which makes the presence of hydroxonium ions improbable.

The base hydrolysis of C₄H₈TeI₂ (**8**) with an excess of aqueous NaOH solution afforded the tritelluroxane diiodide (C₄H₈Te)₃O₂I₂ (**9**) in excellent yield as colourless crystals



The molecular structure and supramolecular association of **9** is shown in Fig. 6. Selected bond parameters and crystal and refinement data are collected in the caption of Fig. 6 and Table 1, respectively. Again, the spatial arrangement around the Te atoms is trigonal bipyramidal. Like in compounds **3** and **5**, the coordination of the terminal Te atoms (Te1 and Te3) is distorted. The average Te–O bond length of Te1 and Te2 (1.94(1) Å) is shorter than the average Te–O bond length of Te3 (2.11(1) Å). The average Te–I bond length of 3.322(2) Å is longer than in C₄H₈TeI₂ (**8**) being 2.925(1) Å [12] and resembles that of **3** and **5**. Besides the primary Te–I bonds, there are a number of secondary

Te···I contacts ranging from 3.636(2) to 4.021(2) Å that connect adjacent molecules in the crystal lattice. Thus, Te1 is involved in one secondary contact, whereas Te2 and Te3 reveal two such contacts. Once crystallized from the mother liquor, the tritelluroxane **9** is virtually insoluble in all solvents, with the exception of methanol where it is sparingly soluble. The ¹H NMR spectrum of **9** reveals two equally intense signals at δ 2.86 and 2.40, which suggest that all C₄H₈Te moieties are magnetically equivalent in solution. Presumably electrolytic dissociation takes place upon dissolution in methanol.

3. Experimental

3.1. General

The diorganotellurium compounds R₂TeI₂ (**1**, R = *p*-MeOC₆H₄ [18]; **4**, R = Me [19]), (*p*-MeOC₆H₄)₂TeO (**2**) [4], Me₂Te(OH)₂ (**6**) [19], C₄H₈TeI₂ (**8**) [20] have been prepared according to literature procedures. The ¹H and ¹³C NMR spectra were recorded using Jeol GX 270 and Varian

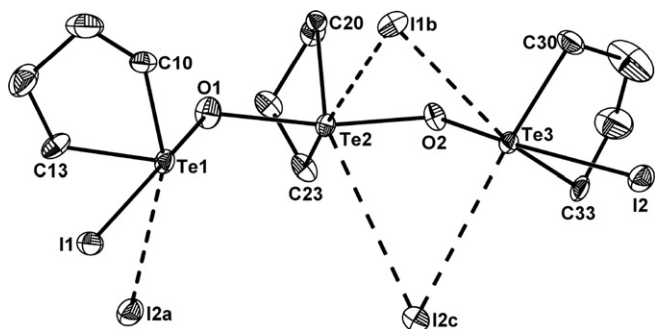


Fig. 6. Molecular structure and supramolecular association of $(C_4H_8Te)_3O_2I_2$ (**9**) showing 30% probability ellipsoids and the crystallographic numbering scheme. Symmetry codes used to generate equivalent atoms: $a = x, 1 + y, z, b = 1 - x, -0.5 + y, 1.5 - z, c = 2 - x, 0.5 + y, 1.5 - z$. Selected bond parameters [Å, °]: Te1–O1 1.93(1), Te1–I1 3.303(2), Te1...I2a 4.021(2), Te1–C10 2.14(2), Te1–C13 2.13(2), Te2–O1 2.16(1), Te2–O2 2.06(1), Te2...I1b 3.662(2), Te2...I2c 3.918(2), Te2–C20 2.11(1), Te2–C23 2.13(2), Te3–O2 1.95(1), Te3–I2 3.341(2), Te3...I1b 3.687(2), Te3...I2c 3.636(2), Te3–C30 2.18(2), Te3–C33 2.14(2); O1–Te1–I1 179.2(4), O1–Te1–C10 93.9(6), O1–Te1–C13 92.7(7), I1–Te1–C10 85.3(5), I1–Te1–C13 87.4(5), C10–Te1–C13 83.6(7), O1–Te2–O2 165.7(5), O1–Te2–C20 82.2(6), O1–Te2–C23 86.4(6), O2–Te2–C20 84.2(6), O2–Te2–C23 88.2(6), C20–Te2–C23 85.5(7), O2–Te3–I2 176.5(4), O2–Te3–C30 92.4(6), O2–Te3–C33 92.0(6), I2–Te3–C30 84.2(5), I2–Te3–C33 87.3(5), C30–Te3–C33 84.4(8), Te1–O1–Te2 115.2(6), Te2–O2–Te3 118.0(6).

300 Unity Plus spectrometers and are referenced to $SiMe_4$ ($^1H, ^{13}C$). Microanalyses were obtained from a Vario EL elemental analyzer. Infrared spectra were recorded using Nexus FT-IR spectrometer with a Smart DuraSamplIR. Raman spectra were recorded using a Bruker RFS 100/S spectrometer with a Nd:YAG laser.

3.2. Synthesis of $[(p-MeOC_6H_4)_2Te]_2OI_2$ (**3**)

A mixture of $(p-MeOC_6H_4)_2TeO$ (0.18 g, 0.5 mmol) and $(p-MeOC_6H_4)_2TeI_2$ (0.30 g, 0.5 mmol) was dissolved in THF (20 mL) and stirred for 1 h. With a minimum of convection, a layer of hexane (30 mL) was carefully placed over this solution. Overnight crystallisation at the layer interface afforded orange crystals of **3** (0.44 g, 0.46 mmol, 92%; m.p. 200–201 °C). 1H NMR ($CDCl_3$): $\delta = 7.84$ (d, 8H, $p-O_oMeC_6H_4$), 6.76 (d, 8H, $p-O_mMeC_6H_4$), 3.75 (s, 12 H, OCH_3). ^{13}C NMR ($CDCl_3$): $\delta = 161.3$ ($p-O_pMeC_6H_4$), 136.8 ($p-O_oMeC_6H_4$), 116.1 ($p-O_iMeC_6H_4$), 114.7 ($p-O_oMeC_6H_4$), 55.3 (OCH_3). Raman: $\tilde{\nu} = 3065w, 3050w, 3015w, 2962w, 2935w, 1583m, 1565w, 1453w, 1433w, 1401w, 1308w, 1254w, 1183w, 1060w, 1000w, 825w, 790s, 702w, 627m, 600s, 590s, 519w, 454s$ cm^{-1} . Anal. Calc. for $C_{28}H_{28}I_2O_5Te_2$ (953.53): C, 35.27; H, 2.96. Found: C, 35.33; H, 2.57%.

3.3. Synthesis of $[(Me)_2Te]_2OI_2$ (**5**)

Solid Me_2TeI_2 (0.41 g, 1 mmol) was dissolved in conc. NH_3 solution (5 mL). Vacuum suction was applied to remove most of the excess NH_3 . Slow evaporation of the

water produced colourless crystals of **5** that slowly turned orange red upon standing at air (0.22 g, 0.38 mmol, 76%; m.p.: 100–102 °C (decomp.)). 1H NMR (D_2O): $\delta = 2.62$ (s, 6H, $^2J(^1H-^{125}Te)$ 26 Hz). Raman: $\tilde{\nu} = 3010w, 2916m, 1400vw, br, 1231m, 1216w, 849vw, br, 654m, 546sh, 536vs, 426vs, 249w, 211sh, 185m, 143m, 115m$ cm^{-1} . Anal. Calc. for $C_4H_{12}I_2OTe_2$ (581.15): C, 8.21; H, 2.07. Found: C, 8.21; H, 1.68%.

3.4. Synthesis of $2 (Me_2Te)_2O(I)OH \cdot H_2O$ (**7**)

To a solution of $Me_2Te(OH)_2$ (prepared *in situ* from Me_2TeI_2 (1.7 g, 4 mmol) [19] in water (20 mL) solid Me_2TeI_2 (0.41 g, 1 mmol) was added. Slow evaporation of the water afforded clear crystals of **7** (310 mg, 0.64 mmol, 64%; m.p. 144–145 °C). 1H NMR (D_2O): $\delta = 2.50$ (s, 6H, $^2J(^1H-^{125}Te)$ 25 Hz). Raman: $\tilde{\nu} = 3028sh, 3009w, 2919m, 1408vw, br, 1237w, 1223w, 1212w, 1016w, 650m, 556s, 546s, 535s, 499m, 470m, 437m, 266m, 219m, 119s$ cm^{-1} . IR: $\tilde{\nu} = 3433m, 3302s, 3221sh, 3032sh, 3005m, 2936sh, 2912m, 1641m, 1402m, 1233m, 1219m, 1209m, 1101m, br, 1015m, 886m, 874sh, 858m, 827m, 811m, 652s, 564m, 546m, 534m$ cm^{-1} . Anal. Calc. for $C_4H_{13}IO_2 \cdot Te_2 \cdot \frac{1}{2}H_2O$ (486.26): C, 9.92; H, 2.91. Found: C, 9.92; H, 2.52%.

3.5. Synthesis of $(C_4H_8Te)_3O_2I_2$ (**9**)

Solid $C_4H_8TeI_2$ (0.72 g, 1.65 mmol) was suspended in methanol (50 ml) and 4 ml of NaOH (5 M) was added. The coloured solution became clear and the remaining iodide dissolved. The reaction mixture was filtered and another portion of the NaOH (2 ml) was added. Slow evaporation of the solvent produced colourless crystals of **9** (0.42 g, 0.5 mmol, 91%; m.p. 185 °C) decomp. 1H NMR (CD_3OD): $\delta = 2.86$ (m, 2H), 2.40 (m, 2H). IR: $\tilde{\nu} = 3422s, br, 3010w, 2989w, 2944m, sh, 2921m, 2854m, 1620m, br, 1449w, 1436m, 1399m, 1389m, 1326vw, 1301m, 1237m, 1230m, sh, 1182m, 1150w, 1140w, 1086m, 1079m, sh, 1041m, sh, 1033m, 957w, 943m, 871w, 853m, 824w, 802m, 756m, 736m, 668s, 599vs, br, 563s, 552s, 532s$. Anal. Calc. for $(C_4H_8Te)_3O_2I_2$ (836.93): C, 17.22; H, 2.89. Found: C, 17.18; H, 2.50%.

3.6. X-ray crystallography

Intensity data were collected on a Bruker SMART 1000 area detector (**3, 1a, 5, 7**) or a STOE IPDS 2T area detector (**9**) with graphite-monochromated Mo $K\alpha$ (0.7107 Å) radiation. Data were reduced and corrected for absorption using the programs SAINT and SADABS [21]. The structures were solved by direct methods and difference Fourier synthesis using SHELXS-97 implemented in the program WINGX 2002 [22]. Full-matrix least-squares refinements on F^2 , using all data. All non-hydrogen atoms were refined using anisotropic displacement parameters. Hydrogen atoms attached to carbon atoms were included in geometrically calculated

positions using a riding model and were refined isotropically. For **7**, the hydrogen atom H4 attached to O4 was located during the refinement and was also refined isotropically. The absolute configuration of **9** was determined by examination of the Flack parameter 0.00(14). Figures were created using DIAMOND [23].

Acknowledgements

Mrs. Irene Brüdgam (Freie Universität Berlin) is thanked for the X-ray data collection. The Deutsche Forschungsgemeinschaft (DFG) is gratefully acknowledged for financial support.

Appendix A. Supplementary material

CCDC 671469, 671470, 671471, 671472 and 671473 contain the supplementary crystallographic data for this paper. These data can be obtained free of charge from The Cambridge Crystallographic Data Centre via www.ccdc.cam.ac.uk/data_request/cif. Supplementary data associated with this article can be found, in the online version, at [doi:10.1016/j.jorganchem.2007.12.006](https://doi.org/10.1016/j.jorganchem.2007.12.006).

References

- [1] (a) J. Zuckerman-Schpector, I. Haiduc, Phosphorus, Sulfur, Silicon 171 (2001) 73;
(b) I. Haiduc, J. Zuckerman-Schpector, Phosphorus, Sulfur, Silicon 171 (2001) 171;
(c) W.-W. du Mont, C.G. Hrib, Handbook of Chalcogen Chemistry (2007) 833;
(d) M.C. Aragoni, M. Arca, F.A. Devillanova, A. Garau, F. Isaia, V. Lippolis, A. Mancini, Bioinorg. Chem. Appl. (2007) 1.
- [2] (a) W.-W. du Mont, H.U. Meyer, S. Kubinoik, S. Pohl, W. Saak, Chem. Ber. 125 (1992) 761;
(b) A.C. Hillier, S.-Y. Liu, A. Sella, M.R.J. Elsegood, Angew. Chem., Int. Ed. 38 (1999) 2745;
(c) D. Witthaut, K. Kirschbaum, O. Conrad, D.M. Giolando, Organometallics 19 (2000) 5238;
(d) H.T.M. Fischer, D. Naumann, W. Tyrra, Chem. Eur. J. 12 (2006) 2515;
(e) J. Beckmann, S. Heitz, M. Hesse, Inorg. Chem. 46 (2007) 3275;
(f) J. Beckmann, M. Hesse, H. Poleschner, K. Seppelt, Angew. Chem., Int. Ed. 46 (2007) 8277.
- [3] (a) E.S. Lang, R.M. Fernandes Jr., E.T. Silveira, U. Abram, E.M. Vázquez-López, Z. Anorg. Chem. 625 (1999) 1401;
(b) P.D. Bolye, W.I. Cross, S.M. Godfrey, C.A. McAuliffe, R.G. Pritchard, S. Sarward, J.M. Sheffield, Angew. Chem., Int. Ed. 39 (2000) 1796;
(c) E.S. Lang, G. Manzoni de Oliveira, R.M. Fernandes Jr., E.M. Vázquez-López, Inorg. Chem. Comm. 6 (2003) 869;
(d) D.B. Werz, R. Gleiter, F. Rominger, J. Organomet. Chem. 689 (2004) 627;
(e) G.N. Ledesma, E.S. Lang, U. Abram, J. Organomet. Chem. 689 (2004) 2092;
(f) E.S. Lang, G. Manzoni de Oliveira, G.N. Ledesma, Z. Anorg. Allg. Chem. 631 (2005) 1524;
(g) J. Beckmann, D. Dakternieks, A. Duthie, C. Mitchell, M. Schürmann, Aust. J. Chem. 58 (2005) 119;
(h) J. Beckmann, D. Dakternieks, A. Duthie, C. Mitchell, Acta Crystallogr., Sect. E61 (2005) o986;
(i) G. Manzoni de Oliveira, E. Faoro, E.S. Lang, G.A. Casagrande, Z. Anorg. Allg. Chem. 632 (2006) 659;
(j) E.S. Lang, G. Manzoni de Oliveira, G.A. Casagrande, J. Organomet. Chem. 691 (2006) 59;
(k) E. Faoro, G. Manzoni de Oliveira, E.S. Lang, J. Organomet. Chem. 691 (2006) 5867;
(l) E.S. Lang, G.A. Casagrande, G. Manzoni de Oliveira, G.N. Ledesma, S.S. Lemos, E.E. Castellano, U. Abram, Eur. J. Inorg. Chem. (2006) 958.
- [4] J. Beckmann, D. Dakternieks, A. Duthie, F. Ribot, M. Schürmann, N.A. Lewcenko, Organometallics 22 (2003) 3257.
- [5] (a) J. Beckmann, D. Dakternieks, A. Duthie, N.A. Lewcenko, C. Mitchell, Angew. Chem., Int. Ed. 43 (2004) 6683;
(b) J. Beckmann, D. Dakternieks, A. Duthie, C. Mitchell, Dalton Trans. (2005) 1563;
(c) J. Beckmann, J. Bolsinger, Organometallics 26 (2007) 3601;
(d) J. Beckmann, J. Bolsinger, A. Duthie, Austr. J. Chem., submitted for publication.
- [6] J. Farran, A. Alvarez-Larena, M.V. Capparelli, J.F. Piniella, G. Germain, L. Torres-Castellanos, Acta Crystallogr., Sect. C 54 (1998) 995.
- [7] M. Suzuki, I.-H. Son, R. Noyori, H. Masuda, Organometallics 9 (1990) 3043.
- [8] J. Beckmann, D. Dakternieks, A. Duthie, N.A. Lewcenko, C. Mitchell, M. Schürmann, Z. Anorg. Allg. Chem. 631 (2005) 1856.
- [9] M.J. Taylor, L.-J. Baker, C.E.F. Rickard, P.W.J. Surman, J. Organomet. Chem. 498 (1995) C14.
- [10] M.J. Almond, M.G.B. Drew, D.A. Rice, G. Salisbury, M.J. Taylor, J. Organomet. Chem. 522 (1996) 265.
- [11] H. Pritzkow, Inorg. Chem. 18 (1979) 311.
- [12] (a) P.C. Srivastava, S. Bajpai, S. Bajpai, C. Ram, R. Kumar, J.P. Jasinski, R.J. Butcher, J. Organomet. Chem. 689 (2004) 194;
(b) P.C. Srivastava, S. Bajpai, R. Lath, R.J. Butcher, J. Organomet. Chem. 608 (2000) 96.
- [13] (a) W. Holzer, W.F. Murphy, H.J. Bernstein, J. Chem. Phys. 52 (1970) 399;
(b) A. Anderson, T.S. Sun, Chem. Phys. Lett. 6 (1970) 611.
- [14] (a) R.H. Vernon, J. Chem. Soc. 117 (1920) 889;
(b) R.H. Vernon, J. Chem. Soc. 119 (1921) 687.
- [15] L.Y.Y. Chan, F.W.B. Einstein, J. Chem. Soc., Dalton Trans. (1972) 316.
- [16] H. Citeau, K. Kirschbaum, O. Conrad, d.M. Giolando, Chem. Commun. (2001) 2006.
- [17] T. Steiner, Angew. Chem., Int. Ed. 41 (2002) 48.
- [18] K. Lederer, Chem. Ber. 49 (1916) 1076.
- [19] (a) R.H. Vernon, J. Chem. Soc. (1920) 86;
(b) P.C. Srivastava, S. Bajpai, C. Ram, R. Kumar, R.J. Butcher, J. Organomet. Chem. 692 (2007) 2482.
- [20] G.T. Morgan, F.H. Burstall, J. Chem. Soc. (1931) 180.
- [21] SMART, SAINT and SADABS, Siemens Analytical X-ray Instruments Inc., Madison, WI, USA, 1999.
- [22] L.J. Farrugia, J. Appl. Cryst. 32 (1999) 837–838.
- [23] DIAMOND V3.1d, Crystal Impact GbR, K. Brandenburg, H. Putz, 2006.